西藏玉龙斑岩铜矿带
花岗岩类与成矿

马鸿文 著

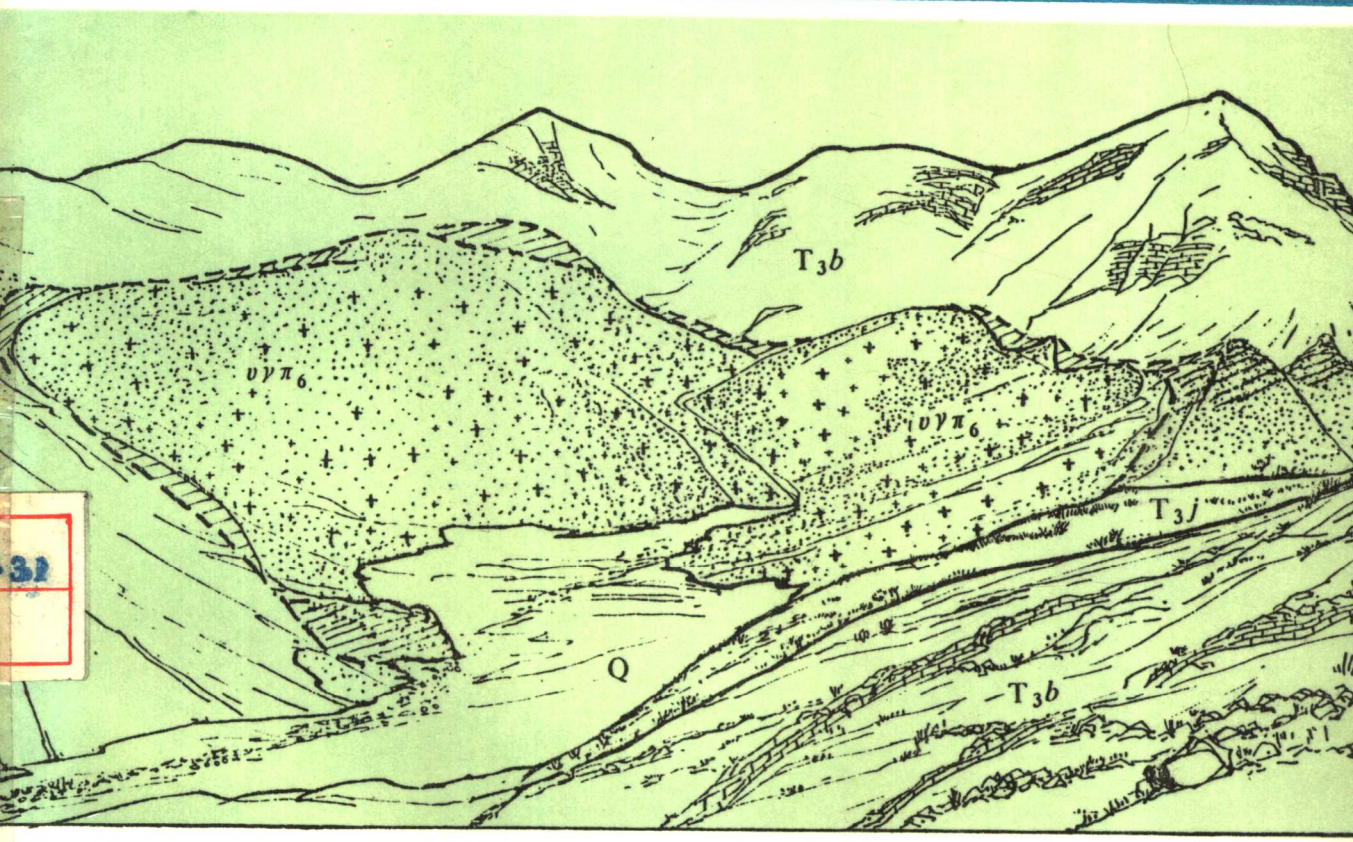

中国地质大学出版社

西藏玉龙斑岩铜矿带花岗岩类与成矿

马鸿文 著

中国地质大学出版社

内容提要

本书在概述西藏东部玉龙斑岩铜矿带成矿地质背景的基础上分析了主要控矿地质因素，从含矿斑岩及有关侵入岩、喷出岩的岩类学、矿物学、全岩化学、微量元素地球化学和同位素研究入手，详细讨论了含矿斑岩的岩石学特征、岩浆活动的时代和地球动力学背景、斑岩的成因类型、成岩成矿物质来源、晚期岩浆至岩浆期后流体相的成因和岩浆作用的物理化学条件。在对岩浆作用与成矿作用成因联系的研究基础上，建立了斑岩含矿性模式和含矿性评价的岩石学标志。

本书可供地质、岩矿、地球化学、矿产地质与勘探和经济地质专业研究人员、高等院校师生、研究生和野外地质勘探人员参考。

*　　*　　*

西藏玉龙斑岩铜矿带花岗岩类与成矿
马鸿文　著

责任编辑：赵俊磊
封面设计：覃功炯
责任校对：郭腊先
中国地质大学出版社出版发行
(武汉市喻家山)
中国地质大学(北京)轻印刷厂印刷　湖北省新华书店经销
开本 787×1092　1/16　印张：11.3　字数：275　千字　印数：1—1000 册
1990 年 5 月第 1 版　1990 年 5 月第 1 次印刷

ISBN 7-5625-0424-5/P·130　国内定价：6.00 元

前　言

西藏东部玉龙斑岩铜矿带是全球性的古特提斯成矿带的一部分．该矿带大致沿金沙江和澜沧江的分水岭地带由北向南纵贯昌都、江达、察雅、贡觉和芒康五县．其分布范围为北纬 29°10′—32°，东经 97°20′—98°40′．北纬 30°50′以北，矿带走向约为 325°，向北西进入青海南部杂多、治多地区，并可能经西乌金兰湖、昆仑山脉一线西延至地中海国家．30°50′以南，矿带走向近南北，延入滇西后走向转为约 150°，经祥云后可能沿红河断裂到达中越国境．

自 20 世纪 50 年代以来在本区作过基础地质工作的主要有以李璞教授为首的中国科学院西藏工作队(1∶50 万路线地质调查，1951—1953)、四川省第三区测队(1∶100 万昌都幅地质矿产调查，1967—1972)和西藏地质一队(玉龙矿带 1∶20 万路线地质调查，1973—1978)．

玉龙矿带的玉龙矿床首先发现于 1966 年．经西藏地质一队二十余年的艰苦工作，迄今在藏东这一南北长约 300km、东西宽 15—30km 的狭长地带已发现并经详查的特大型斑岩铜矿床一处(玉龙)、大型矿床两处(马拉松多、多霞松多)，经初查的中、小型矿床各一处(莽总、扎那尕)，未经普查的矿(化)点数处．其中玉龙矿床储量之大、品位之富、蚀变-矿化分带之完整，为我国同类矿床之首，按铜的金属量，居世界第十一位，矿床地质特征也可与世界上典型的斑岩铜矿床相类比．

对该矿带斑岩铜矿先后作过较系统的科研工作的主要有西藏地质一队、成都地质矿产研究所，中国地质科学院矿床所及地质所等单位，但各家对矿床成因、含矿斑岩的成因类型、岩浆侵入时代以及成岩成矿物质来源等关键问题的认识尚有争议．

本专著是池际尚教授主持完成的国家教育委员会《岩浆岩与成矿的关系》科研项目(1982—1985)的一部分．作者在西藏地质一队的协助下，先后于 1980 年和 1983 年完成了对研究区 22 个喜马拉雅期浅成至超浅成侵入体和部分喷出岩的野外地质调查，并在对其中 16 个侵入体和部分喷出岩进行室内研究的基础上，分别于 1982 年和 1986 年提交了题为《藏东马拉松多铜矿区斑岩岩石学及其与成矿关系的研究》的硕士论文和题为《藏东玉龙铜矿带斑岩岩石学与含矿性研究》的博士论文．本书即是在上述工作基础上对所获资料作进一步综合整理完成的．

本项研究旨在通过详细的岩石学、矿物学、全岩化学、微量元素地球化学和同位素研究，在查明研究区花岗岩类岩石学特征的基础上，追溯岩浆演化史、研讨岩浆作用与成矿作用的内在联系，建立该区斑岩含矿性模式和含矿性评价的岩石学标志．作者希望所获研究成果对在藏东地区进一步普查和勘探斑岩型铜矿有所裨益，并对在其它地区寻找"玉龙式"铜矿有借鉴意义．

本项研究是在池际尚教授的指导下完成的．工作中得到西藏地质一队张明亮高工、唐仁鲤高工、李建成、文洪安、刘玉榕、郭天成、旺秋、杨善清等几位工程师和我校邓晋福教授、孙善平教授、周珣若教授、路凤香教授、赵崇贺副教授、莫宣学副教授、邵道乾副

教授和任迎新老师等的关怀、指点和帮助．本书初稿承蒙池际尚教授和路风香教授审阅，以及宋叔和研究员、吴利仁研究员和朱上庆教授评审，张本仁教授、翟裕生教授和周珣若教授曾审阅了原稿的部分内容，路风香教授和莫宣学副教授审阅了修改稿．他们所提出的许多宝贵意见和建议避免了书中不少错误或疏漏之处．书中图件由我校(北京)绘图室清绘．本项研究主要由国家教育委员会的博士导师科研经费资助．在此一并致谢．

作　者

1989.5

PETROLOGY AND MINERALIZATION OF GRANITES IN YULONG PORPHYRY COPPER BELT, TIBET

MA Hongwen (马鸿文)

(*China University of Geosciences, Beijing* 100083, *PRC*)

ABSTRACT

I. GEOLOGICAL SETTING

Yulong porphyry copper belt, the largest one in China, is located at the eastern margin of the Tibet plateau, with latitude 29° 10′–32° N and longitude 97° 20′–98° 40′E. Tectonically it is a part of the Paleo–Tethysian metallogenic province, and elongates parrallel to Jinshajiang fault representing subduction zone of the Paleo –Tethysian ocean plate (Fig.1–1), which is believed to be formed during the Indosinian movement.

Strata occurring in the Yulong belt are mainly Palaeozoic and lower Mesozoic, i. e. flysch clastic rocks of lower Ordovician (O_1w), marine carbonates of middle Devonian to Permian, intercalated with intermediate volcanic rocks at top, dacitic to rhyolitic lava and pyroclastic rocks of lower Triassic, and nonmarine–littoral carbonates and clastic rocks. Nonmarine clastic rocks of Jurassic to Cretaceous are exposed on the west of the copper belt, and those of lower Tertiary on the east, hence a anticlinorium along the copper belt (Fig.1–3).

Granite porphyries emplaced during the early Tertiary mainly as small stocks with surface area less than $1km^2$. All porphyries hosting copper mineralizations and most of porphyries barren in copper were localized at the near axial positions of subordinate anticlines, with various country rocks, showing a close correlation between the regional structural events and the magma emplacements. Airborne magnetic survey data show a linear positive anomaly along the copper belt (Fig.1–5), indicating that these bodies may be offshoots of an elongated batholith at depth.

Ore deposits in the Yulong belt are all hosted by granite porhyries and the nearby country rocks with veinlet–disseminated ore structure. Where carbonates occur as country rocks, massive sulfide ore was formed. Primary ore minerals include chalcopyrite, pyrite, molybdenite, bornite, and magnetite. Metals such as Au, Ag, Re, Fe, S, and platinum group can be economically utilized in addition to Cu and Mo. Copper reserves of the deposits tend to increase with increasing Au / Cu, $\sum$ Pt / Cu, and Cu / Mo ratios (Fig.1–6).

Major controlling factors over the porphyry copper mineralizations: 1) the geographical distribution of the copper belt is controlled by the deep level geochemistry; 2) the emplacemental locations, by the shallow level structure, i.e. simultaneous regional structur-

al stress field; 3) the porphyry copper mineralizations mainly by the relevant magma processes; and 4) the copper reserves, to some extent, by the nature of rock- and ore-forming source materials.

II. GEOLOGY OF THE INTRUSIVE BODIES

The Yulong copper belt is essentially composed of hypabyssal to ultra-hypabyssal granite porphyries. The following porphyry bodies hosting copper mineralizations have been studied, i.e., Xiariduo, Hengxingcuo, Yulong, Zhanaga, Mangzong, Duoxiasongduo, Malasongduo, Gegongnong, Seli, Mamupuxi from north to south (Fig.1-3). Also studied in some detail are copper-barren plutons such as Randala, nearby Yulong pluton swarm, Secuo, Riqu, Riqunan, and Mamupudong. Geological features of 17 major intrusive bodies are listed in Table 2-1. Those porphyry bodies detailedly described in the text include Yulong (Fig.2-1 to 2-3). Malasongduo (Fig.2-4), Duoxiasongduo (Fig.2-5), Zhanaga (Fig.2-6), and Mamupu (Fig.2-7). All of them have rather well been investigated and explored.

Character analysis method has been adopted to extract principal characteristics from 34 selected geological features for both copper-bearing and -barren intrusive bodies, which include occurrence, surface shape, exposed area, and structural locality of the intrusive bodies, texture, rock type, and hydrothermal alteration of the granites, and chronology, lithology, and alteration of country rocks etc. Getting through the vector length analysis of the 34 geological features of 12 copper-bearing and 28 copper-barren intrusive bodies in the Yulong belt, the following remarks can be made.

Geological marks of copper mineralizability: 1) the occurrences of the intrusive bodies are mainly near circular stocks exposed mostly less than $1km^2$, and emplaced at ultra-hypabyssal level ($<1.5km$); 2) the intrusive bodies typically emplaced in subordinate anticlines; 3) the rock type are mainly monzogranite, syenogranite, and alkali-feldspar granite porphyries; 4) zonal hydrothermal alteration halos were developed around the intrusive bodies and the surrounding country rocks; and 5) the copper-bearing bodies are mostly multistage intruded composite complexes. Another item can be added to the copper-bearing bodies is their network vein structure, and even explosive breccia in some plutons.

III. PETROGRAPHY

Cluster analysis method has been used to classify the granites based on analyses of 56 major and trace element concentrations of 43 samples. The result shows that the granites can be divided into three groups according to similarity coefficients (Fig.3-1). All samples from copper-bearing plutons and related copper-barren ones, by geological criteria, fall into group one and group two, while lavas with various ages, samples from other copper-barren plutons, and country rocks among others into group three. It is likely that

the magmatism to give rise to granites of the group one and two were responsible for the copper mineralizations in the area. Thus the current research is concentrated on petrography and petrogenesis of the granites in those two groups, with special reference to the relationships between the magma processes and mineralizations, particularly to the marks of copper mineralizability in the area studied.

The granites in the Yulong belt are mostly light-gray, gray to grayish white coloured, massive structured, and porphyry textured with 30–50% phenocrysts of hornblende, biotite, andesine to oligoclase, sanidine to intermediate microcline, and quartz. The groundmasses are microgranular or micropoikilitic textured, and composed of oligoclase to albite, sanidine to orthoclase, and quartz. Major accessory minerals are magnetite, apatite, and zircon with or without sphene.

Based on ANOR–Q′ parameter classification scheme (Strekeisen et al, 1979) the granites in the area are classified into several rock types such as monzogranite, syenogranite, alkali–feldspar granite, and alkali–feldspar syenite porphyries, which are both ore–bearing (Fig.3–2a) or free from ore (Fig.3–2b). The granites in the Yulong belt are more alkalic than those in the Cordilleran copper belt (Hollister, 1978) (Fig.3–3), and also more alkalic and silicious than those in Dexing porphyry copper area in south China (circles in Fig.3–2a). Although rock type seems not to be a principal controlling factor over porphyry copper mineralizations in the Yulong belt, the scale of copper reserves tends to decrease from monzogranite porphyry (Yulong), through syenogranite porphyry (Angkenong), to alkali–feldspar granite porphyry (Duoxiasongduo) (Fig.1—6).

Petrographic marks of copper mineralizability: 1) the copper mineralizations in the Yulong belt are hosted by monzogranite, syenogranite, alkali–feldspar granite, and alkali–feldspar syenite porphyries; 2) rock type is not a principal controlling factor over porphyry copper mineralizations, but ore reserves show a tendency to decrease with decreasing basicity of the host rocks; 3) host rock type can vary from one copper province to another, indicating that porphyry copper mineralizations are mainly constrained by geochemical background of the regional magmatic processes.

IV. MINERALOGY

Hornblende: It only occurs as dark green euhedral phenocryst in monzogranite porphyry (Photo 1), with pleochroism Ng = green, Nm = light green, and Np = light yellow. Polysynthetic twins and occasionally zonal structure are observed. Based on 10 microprobe analyses (Tab.4–1, 2) X_{Fe}/X_{Mg} ratios of hornblendes from the copper–bearing plutons vary from 0.42 to 0.59, while those from the copper–barren ones from 0.63 to 0.85, with similar X_{Al}/X_{Si} ratios (=0.14–0.24) for the both. It is found that X_{Fe}/X_{Mg} and X_{Al}/X_{Si} ratios are closely correlated each other, indicating that substitutions of Fe for Mg and Al for Si are probably coupled.

Biotite: It is present in nearly all samples studied as euhedral phenocryst, with

pleochroism $Ng \approx Nm$ = brown to dark brown, and Np = yellow to light yellow. Zircon and apatite are commonly found in biotite phenocrysts as inclusions. Based on wet chemical analyses the biotites fall into meroxene (Fig.4–5), and the correlation within Fe^{3+}–Fe^{2+}–Mg compositional triangle (Fig.4–4) suggests that compositions of the biotites are defined by oxygen fugacities close to those of the NNO buffer. Both chemical and microprobe analyses show that the biotites from the copper–bearing plutons have X_{Mg} ranging from 0.666 to 0.741, compared with those from the copper–barren ones (X_{Mg} = 0.583–0.652). Considerable amount of chlorine is detected in the biotites (Tab.4–3), particularly in those from the copper–bearing plutons, suggesting that the biotites might be equilibrated with chloride–rich vapor phase to which it was attributed to transfer copper from the magmas into hydrothermal fluids and, in turn, to cause copper mineralizations. A positive correlation between X_{Fe} / X_{Mg} and X_{Al} / X_{Si} ratios of the biotites is also found (Fig.4–6), indicating that, as in hornblende, the substitutions of both Fe for Mg and Al for Si are probably also coupled in biotites.

Calculations of best fit to X–ray powdery diffraction data (Tab.4–5) show that the biotites are all $2M_1$ polytype with cell parameters of a = 5.331–5.397 Å, b = 9.222–9.254 Å, c = 20.161–20.253 Å, β = 94° 47′–95° 07′, and v = 987.40–1006.128 Å^3, each of which is a linear function of the biotite chemistry, Mössbauer spectra (Tab.4–6) are computer fitted to Lorentzian line shapes and consisted of two doublets arising from Fe^{2+} in the two non–equivalent octahedral sites of M_1 and M_2 and two doublets due to Fe^{3+}. Ferric concentrations are obtained in accordance with wet chemical analyses (Fig.4–7). Treating biotite as a Fe^{3+}–Fe^{2+}–Mg ternary solid solution, site occupancy assignment shows that over about 95% of M_1 site are occupied by Fe^{3+}, Fe^{2+}, and Mg, while only 76–85% of M_2 site by them, indicating that Ti, Al^{VI}, Mn and vacancy are probably held mainly in M_2 site.

Feldspars: Both plagioclase and K–feldspar are present as euhedral phenocrysts and hypidiomorphic to allotriomorphic–granular crystals in groundmass of the porphyries. The plagioclases develop albite twin, Calsbad and albite composite twin, and occasionally cathrate twin, and orthoclase Carlsbad twin. Zonal structure is observed in plagioclase, and rarely sanidine. Microprobe analyses show that both plagioclase and K–feldspar can be divided into several populations (Fig.4–11, 12). The plagioclase phenocrysts are An_{40-29}, and An_{29-18}, and groundmass An_{20-16}, and An_{12-4}, with a gap between An_{16} and An_{13}, which might arise from temperature drop of crystallization (Fig.11–3). The K–feldspar phenocrysts are mainly Or_{79-60}, and groundmass Or_{91-82}, probably due to p_{H_2O} increasing to cause more Or–rich sanidine and orthoclase crystallized in groundmasses (Fig.11–3). The Al / Si ordering of K–feldspar phenocrysts in the copper–bearing porphyries are more developed than those from the copper–barren ones (Fig.4–18, 19), partially because the former might capture a small amount of H_2O to compose SiO_3OH (Tab.4–10, Fig.4–22),

which would enhance the process of Al / Si ordering. Within a single pluton Al / Si ordering degree tends to decrease outwards and upwards (from $\theta = 0.55-0.65$ to $\theta = 0.30-0.40$) (Fig.4–21). Some feldspars in groundmasses are detected to have excess silica than stoichiometry. Taking feldspar as a An, Ab, Or, and $\square Si_4O_8$ solid solution substitution of $\square Si_4O_8$ for (Ca, Na, K) $Al_{2-1}Si_{2-3}O_8$ can reach 40% or so by the present data (Fig.4–23, 24).

Accessory Minerals: Major accessory minerals are magnetite, apatite, zircon, rutile, allanite, and sphene. Sphene is only present in monzogranite and alkali–feldspar syenite porphyries as microphenocrysts and in granodiorite. Magnetite is the most abundant accessory mineral, and nearly pure Fe_3O_4variety (Tab.4–13). Apatite is mostly fluor–apatite. The early magmatic apatite is usually long prismatic, and inclosed in biotite and plagioclase phenocrysts, while hydrothermal apatite mostly granular, and distributed throughout. Zircon, the earliest crystallized mineral, is commonly prismatic, and often present in phenocrysts (Photo 16). Sulfide microinclusions such as pyrrhotite and chalcopyrite are found in zircon as inclusions (Photo 20, 21, Tab.4–17), indicating that during early stage the magmas related to the copper mineralizations afterwards might be oversaturated with respect to sulfide. Correlation of sphene occurrence with bulk compositions shows that the stability of sphene is to a great extent depended on concentrations of TiO_2 and CaO relative to SiO_2 (Fig.4–25).

Mineralogical marks of copper mineralizability: 1) X_{Fe} / X_{Mg} ratio of hornblende is less than 0.61, X_{Mg} of biotite is greater than 0.66, and X_{Mg} of biotite tends to increase from core to rim of a single biotite phenocryst for the copper –bearing porphyries; 2) Al / Si ordering degree of K–feldspar is $\theta \geqslant 0.42$, and $Sm \gtrsim 0.36$. K–feldspar phenocrysts fall into orthoclase series with slight transition to intermediate microcline for the copper–bearing porphyries, compared with sanidine series with slight transition to orthoclase for copper–barren porphyries; and 3) sulfide inclusions are present in the early crystallized minerals of the copper–bearing porphyries.

V. BULK CHEMISTRY

Based on 172 bulk rock analyses the granites in the Yulong copper belt are mostly included in calc–alkali series, with Rittman index σ ranging mainly from 1.8 to 3.3 (Fig.5–1). The granites are characterized by lower SiO_2 and Fe_2O_3, and higher Al_2O_3, MgO, and K_2O (Fig.5–2), compared with the average andesite, dacite, and rhyolite (Le Maitre, 1976). With increasing differentiation SiO_2 and K_2O contents of the granites tend to increase, while Al_2O_3, FeO, MgO, and CaO to decrease (Fig.5–2). The higher contents of Al_2O_3, MgO, K_2O, and F (Fig.5–4) might come from breaking down of phlogopite during partial melting of the source rocks.

There exist three distinct metallogenetic belts in the Jinshajiang–Lancangjiang–Nujiang area, i.e. Jiaduoling porphyrite iron belt, Yulong porphyry copper belt, and Chayu

porphyry tin belt. It can be seen from Fig.5–5 that from iron, through copper, to tin mineralizations SiO_2 contents of the host rocks vary mainly from 59–67w_B%, through 64–72w_B%, to 68–76w_B%, indicating that the mineralizations are to a great extent controlled by bulk composition of the magmas, hence by geochemistry of the source rocks and physicochemistry of the magmatic processes. Discrimination analysis shows that the Fe, Cu, and Sn–bearing plutons can be distinquished by bulk composition of the host rocks at 90% confidence level (Tab.5–2, 3).

Judging from correlation coefficients of copper with major components of the host rocks, the copper enrichment is to a great extent controlled by (1) extraction of copper from the magmas to produce copper–rich hydrothermal fluid; (2) replacement of plagioclase by K–feldspar, during which Na^+would be released to raise concentration of NaCl in the fluid, thus to enhance the extraction of copper, and (3) pouring sulfur into the hydrothermal systems at the late stage, thus to promote the precipitation of copper.

Chemical marks of copper mineralizability: 1) iron, copper, and tin mineralizations in the tectonomagmatic belts are obviously controlled by bulk chemistry of the host rocks, the potential copper mineralizability of a pluton, therefore, mainly by composition and structure of the magma; 2) enrichment of copper is mainly controlled by extraction of copper from the magma by hydrothermal fluid rich in chloride, and the concentration of sulfur in the magma–hydrothermal systems.

VI. GEOCHEMISTRY OF TRACE ELEMENTS

Listed in Tab.6–1 are the trace element concentrations of the granites from the Yulong copper belt. Compared with trace element concentrations of the average granitoid (Виноградов, 1962), the granites are characterized by higher concentrations of Sr, Ag, Hf, W, Pb, Bi, Th, and U.

Trace element analyses of 51 phenocrystal samples show that the copper concentration of each phenocryst, including hornblende, biotite, plagioclase, K–feldspar, and quartz, from the copper–bearing plutons is commonly higher than that of the same phenocryst from the copper–barren ones, indicating that the extraction of copper from the solidified host rocks at shallow level, unlike that from the magmas, might be of little significance in contributing copper to mineralizations.

The granites show a LREE–rich, and slightly Eu–negative anomaly pattern (Fig. 6–3). The HFS element concentrations follow the evolutionary path of the Andean–type arc magmas (Fig.6–11) Several plots such as Ce^* / Yb vs. Eu^* / Yb, Ce vs Eu, Sr vs. Rb, Th vs. U, and Pb vs. Th suggest that magma mixing might be involved in the magma evolutions (Fig.6–4, 5, 8, 9, 10). It can also be deduced from Tab.6–13 that from Yulong, through Angkenong, to Duoxiasongduo plutons the major element contents along with most trace element concentrations and ratios indicate a magmatic differentiation trend, while Hf concentration, Zr / Hf, and Th / U ratios require a mixing by a melt higher in

SiO_2 from a depleted acidic granulite source. The data also show that from Yulong, through Angkenong, to Duoxiasongduo, scale of the deposits tends to decrease with increasing differentiation of the deep source I-type magma and hybridization of the magma by shallow S-type partial melts higher in SiO_2. This is also in accordance with decreasing $\sum$ Pt / Cu and Au / Cu ratios, and increasing Mo / Cu ratio of the deposits (Tab.6-13, Fig.1-6).

Trace element marks of copper mineralizability: 1) phenocrysts in the copper-bearing plutons show relatively higher copper concentration; 2) Li, Rb, and Th concentrations of phenocrysts tend to increase, while Sc, Cu, and Zn to decrease, with decreasing scale of the deposits; 3) scale of the deposits tends to decrease with increasing Li, Rb, Pb, Th, U, and Bi concentrations and Rb / Sr, Rb / Ba, Zr / Hf, Th / U, and Mo / Cu ratios of the host rocks, and decreasing Sr, Ba, Hf, Sc, V and Co concentrations and Ba / Pb, Au / Cu, and $\sum$ Pt / Cu ratios, hence with increasing differentiation and hybridization of the I-type magmas by S-type partial melts.

Ⅶ. CHRONOLOGY

Listed in Tab.7-1 are K-Ar apparent ages of 11 granitic plutons in the Yulong copper belt. They clearly cluster around three peak ages (Fig.7-1), i.e., by mean value and standard deviations, 52.0 ± 2.8Ma (55.0-48.2Ma, $n=5$), 40.1 ± 1.3Ma (41.5-37.9Ma, $n=11$), and 33.2 ± 1.3Ma (34.6-30.9Ma, $n=6$) . The Rb-Sr isochronal method gives the Yulong body 52.0 ± 0.2Ma, with initial $^{87}Sr/^{86}Sr$ ratio equal to 0.7066 ± 0.0001, based on 6 whole rock and 4 mineral samples (Tab.7-2). The $^{40}Ar-^{39}Ar$ method gives phenocrystic biotite from the Yulong body apparent age 52.84 ± 1.68Ma. The U-Pb isochronal method gives zircon from the Angkenong body $^{207}Pb-^{235}U$ isochronal age 40.9Ma, and $^{206}Pb-^{238}U$ age 33.7Ma (Tab.7-3, Fig.7-2). These results are in excellent accordance with the three peak ages by K-Ar method, indicating that the magma emplacements in the Yulong belt can be divided into the early, the intermediate, and the late stages.

It is observed that the K-Ar apparent ages of the Yulong body have two peak values, i.e.52.0 ± 2.8Ma and 40.1 ± 1.3Ma as shown in Fig.7-1. These can not be attributed to analytical errors, because the discrepancy is much greater than the uncertainty limit of the method. This phenominon may, therefore, be a result of multiple emplacements of the magma. This is also the case for the Angkenong body, and probably for the Duoxiasonduo body from the available data.

The scale of the deposits tends to decrease from the early, through the intermediate, to the late stage of the magmatism in the area, as the case from Yulong (52.0Ma+40.1Ma), through Angkenong (40.9Ma +32 4Ma), to Duoxiasongduo body (30.9Ma+25.0Ma?).

Chronological marks of copper mineralizability: 1) the magma emplacements in the Yulong belt can be divided into the early, the intermediate, and the late stages; 2) the major copper-bearing plutons are mainly multi-complexes formed by multiple concealed em-

placements of the magmas; and 3) the scale of the deposits tends to decrease with the lapse of the magma emplacemental ages.

Ⅶ. GEODYNAMICS OF THE MAGMA PROCESSES

The granites from the Yulong copper belt, according to bulk composition, are affiliated with volcanic arc magmatisms. They are also inherently related to the Jiaduoling diorite porphyrites hosting iron mineralizations (Fig.8–1, 2), which are believed to be derived from partial melting of the subducted Paleo–Tethysian ocean plate along the Jinshajiang during the Indonisian period. Combined with the data on correlation of copper–molybdenum mineralizations and bulk composition of the host rocks in the convergent plate margin of British Columbia (Griffiths et al, 1983), it is outlined that the complete zoning of metal mineralizations in margin of a convergent plate (island arc) is Fe →Cu→Mo from the suture to the continent.

Trace element data and LILE pattern show that the granites from the Yulong belt are comparable with volcanic arc granite (VAG, Pearce et al, 1984), with relatively higher Rb concentration (Fig.8–3, 4), which can be explained as being dissociated from the source phlogopite. Lead isotopic composition of the granites is also consistent with the average lead isotopic composition for typical orogenic belt (Fig.8–5) (Doe et al, 1979).

Tectonic environment marks of copper mineralizability: 1) Himalayan granitic magmatisms in the Yulong copper belt were developed on a background of the Indonisian volcanic arc of the Paleo–Tethys along the Jinshajiang, and related to inherited activities of the Paleo–Tethysian subduction zone induced by large–scale subduction of the Leading –Tethysian and the Neo–Tethysian ocean plates along Bangong Lake–Nujiang and Yarlun Zangbo respectively during Cretaceous to early Tertiary periods. An inherited island arc can produce volcanic arc granite (VAG) geochemically similar to those in high–maturity island arcs and host porphyry–type copper deposits; 2) the idealized schema of magmatism and the associated metal mineralizations in an island arc is Fe→Cu→Mo from suture to the continent with maturing the arc and lapse of the magmatisms.

Ⅸ. GENETIC TYPE OF THE GRANITE PORPHYRIES

The granites in the Yulong copper belt consist of biotite (meroxene), plagioclase, K–feldspar, and quartz, with hornblende and sphene microphenocrysts mainly in monzogranite porphyry. Magnetite is the major variety among iron–titanium oxide minerals, and ilmentite is rarely found in the granites. This is in accordance with mineral assemblage commonly for I–type or magnetite–series granitoid (Hine et al, 1978; Ishihara, 1977).

Geochemically, the granites have S/I index [Al_2O_3 / ($CaO+Na_2O+K_2O$)] mostly less than 1.1 (Fig.8–2), which is distinctive for I–type granitoid (Hine et al, 1978). Trace element concentrations of the granites are also characteristic of I–type granitoid, except slightly higher Cr and Ni (Fig.9–1, 2). It is noticed that the granites in the Yulong copper belt

have relatively higher K_2O relative to Na_2O, compared with those of typical I–type granitoid such as Kosciusko batholith in Australia (Hine et al, 1978), which is probably controlled by dissociation of near liquidus philogopite in the source rocks.

Isotopically, the granites have $\delta^{34}S$ (‰) ranging from −5.0 to +5.5, the Yulong body has initial $^{87}Sr/^{87}Sr$ ratio equal to 0.7066± 0.0001, again resembling I–type granitoid ($\delta^{34}S$ (‰) =−3.6~+4.2, Coleman, 1979; initial $^{87}Sr/^{86}Sr < 0.708$, Beckinsale et al, 1979).

Oxygen fugacity of the magma processes in the Yulong belt closely followed that defined by NNO buffer during the early magmatic stage, and slightly higher than that during the magma solidification, as defined by Fe_2O_3/FeO ratio in the Yulong monzogranite porphyry (Fig.4–4, Fig.11–1, 4), indicating that the granites fall into magnetite–series granitoid.

Genetic type marks of copper mineralizability: 1) the granites in the Yulong copper belt belong to I–type or magnetite–series granitoid; 2) I–type granitoid is equivalent to magnetite–series one for the granites hosting copper, gold, and molybdenum mineralizations, as the case in the Yulong porphyry copper belt; 3) copper, gold, and molybdenum mineralizations are closely related to I–type or magnetite granitoid.

X. MATERIAL SOURCES

Geochemically, the granites in the Yulong copper belt are characterized by relatively higher Al_2O_3, MgO, K_2O, Rb, and F contents, indicating a phlogopite–bearing fertilized mafic source. This is supported by finding of lamprophyre containing more than 30% phlogopite in the area, which might be an initial magma to cause partial melting of mafic rocks in the lower crust to produce the copper–bearing magmas. The higher $(Ce/Yb)_N$ ratio of the granites is also considered a clue of magmas primarily derived from the mantle (Fig.10–1).

The Yulong body has initial $^{87}Sr/^{86}Sr$ ratio equal to 0.7066± 0.0001. That of the Angkenong body is inferred to be 0.7077 based on Rb–Sr isotopic measurement of K–feldspar phenocryst, and the Duoxiasongduo body, 0.7079. Source material proportions of the granites are estimated based on strontium isotopic data, combined with lead isotopic compositions. The result shows that the granites could be derived over 48–24% from the mantle, and 52–76% from lower crust, or 81–72% from mantle, and 19–28% from upper crust, or any combinations of these two limits.

Lead isotopic compositions of the granites follows the normal lead evolutionary path (Fig.10–3), but within ^{206}Pb–^{207}Pb–^{208}Pb triangle lead isotopic compositions of the bulk rocks show a tendency to enrich in ^{206}Pb, while that of sulfides to enrich in both ^{206}Pb and ^{207}Pb, with decreasing scale of the deposits, from Yulong, through Angkenong to Duoxiasongduo (Fig.10–4). This tendency is concordant with increasing initial $^{87}Sr/^{86}Sr$ ratios of the granites.

Sulfur isotopic compositions of the granites show relatively limited $\delta^{34}S$ (‰) values

ranging from −0.5 to +5.5, which is linearly correlated with biotite Fe_2O_3 / FeO ratios of the granites (Fig.10−5), indicating that the sulfur isotopic compositions might be closely controlled by oxygen fugacity of the magma processes. Thus the slight positive deviation from zero of sulfur isotopic compositions could be attributed to relatively higher oxygen fugacity, and the sulfur was mainly derived from a homogeneous sulfur reservoir, i. e., the mantle or lower crust.

Based on oxygen isotopic fractionation between quartz and water, $\delta^{18}O(‰)$ of the initial magmatic water equilibrated with quartz phenocrysts in Yulong body is about +8.5. Oxygen and hydrogen isotopic compositions, i. e., $\delta^{18}O(‰)$ and $\delta D(‰)$ of the surface water in the area is −18.21 and −135.64 respectively. Using simple two end member mixing model, calculated meteoric water proportions in the hydrothermal fluids at each alteration and principal mineralization stage is 11−20% for K−feldspar + biotite alteration, 18−29% for quartz + sericite alteration, 31−34% for clay alteration, 44−57% for chlorite + epidote +carbonate alteration, and 16−21% for principal vein sulfide precipitation. Estimated δD (‰) of the initial magmatic water is −80 to −85. These results show that the hydrothermal fluids during the principal copper mineralization stage might be mainly separated from the magmas.

Material source marks of copper mineralizability: 1) both rock− and ore −forming material might be derived from upper mantle or lower crust, and hydrothermal fluids during the principal copper precipitation stage might consist mainly of magmatic water, with less than 21% meteoric water mixed; 2) both strontium and lead isotopic data suggest that the scale of the deposits tends to decrease with decreasing proportions of deep source material from upper mantle or lower crust to that from upper crust for an ore−forming magma.

XI. PHYSICOCHEMICAL CONDITIONS OF THE MAGMA PROCESSES

Two−feldspar geothermobarometer method (Ghiorso, 1984) is applied to meladiorite and gneissic biotite syenite xenoliths to estimate geothermal gradient in the area. The calculated geothermal gradient during the early Tertiary was 31.2−32.5℃ / km. Homogeneous temperature measurements of glass inclusions give estimated liquidus temperature as high as 1050−1200℃ . Thus the magmas responsible for the copper mineralizations might be originated from a source deeper than 32.3−38.5km, hence a transitional zone between the mantle and crust, as the huge−thick crust of the Tibetan plateau had not been made up then.

Using various geothermo− and barometers p−t path of the magma processes is traced as: hornblende phenocrysts were crystallized at $p=(2-3)\times 10^8$Pa (Hollister et al, 1987) and $t=910-990$℃ (Helz, 1979); biotite phenocrysts at $p_{H_2O}=(1.4-3.6)\times 10^8$Pa (Wones, 1972) and $t=860-960$℃ (Wones et al, 1965); early zonal plagioclase phenocrysts at $p_{total}>5\times 10^8$Pa and $t=690-740$℃; and groundmassic two−feldspars at $p_{H_2O}=(3.8-5.1)\times 10^8$Pa and

t=630–650℃ (Ghiorso, 1984; Tab.11–2, Fig.11–3). Temperature at which K–feldspar phenocrysts persisted in their structural state, estimated by Al occupancy (Ma Hongwen, 1988), is 650–690℃, about 12 –16℃ above solidus of the granites.

Oxygen fugacity of the magma crystallizations during the early stage closely followed that defined by NNO buffer (Fig.4–4, Fig.11–1), while that at the solidus temperatures was about two log units higher than NNO buffer, as defined dy Fe_2O_3 / FeO equilibrium for the Yulong body, giving a t–$\log f_{O_2}$ path from 860–960℃ and −11.0± 1.0 to 630–650℃ and −15.0± 1.0 (Fig.11–4).

The solubility of water in the melts equilibrated with biotite+zonal plagioclase +magnetite is calculated with the modified Nicholls (1980) method as X_{H_2O} = 0.083 – 0.325 (2.4 –11.7 w_B%) and X_{OH} = 0.114–0.156 (Ma Hongwen, 1985). The fugacity and solubility of sulfur in the copper–bearing magma systems are $\log f_{S_2}$ = 1.33–1.59± 0.54, and X_S = 0.014–0.033 (mol%) (67–158ppm), compared with $\log f_{S_2}$ probably less than −0.6± 0.6, and X_S = 0.002–0.008 (mol %) (12–40ppm) for the coper–barren magma systems.

Microprobe analyses of single biotite phenocrysts show that the Mg / Fe ratio tends to increase from core to the rim of a biotite phenocryst for the copper–bearing plutons, while that to decrease for the copper–barren ones (Tab.11–5), suggesting that during the early crystallizing stage the activity of FeO in the copper–bearing magmas tends to decrease, while that in the copper–barren ones to increase. This might be attributed to that in the copper–bearing magma systems, the higher fugacity and solubility of sulfur might have caused the activity of FeO to be bufferd through the following equilibrium:

$$\text{FeO (silicate melt)} + 1/2S_2 = \text{FeS (sulfide melt)} + 1/2O_2$$

This explanation is supported not only by the sulfur solubility data (Tab.11–3), but also by the occurrence of sulfide microinclusions in the early crystallized minerals of the copper–bearing porphyries (Photo 20, 21). In addition, the ore –forming metals could not be transported by aqueous phase during the early magmatic stage, as the magmas had been undersaturated with water until sulfide drops (microinclusions) were separated from the magmas.

In the Yulong belt the ore–forming material shows a consanguineous relationship with the porphyry magmas; Cu, Au, and Ag concentrations of the porphyries are closely correlated with each other (Tab.6–12); and a Au content as high as 0.437w_B% (0.082–0.726w_B%) and a Ag content of 0.115w_B% (0.000–0.291w_B%, by 8 analyses) are detected in pyrrhotite microinclusions. It is thus infered that the magmas might have been the main carrier of metals such as Cu, Au, and Ag during the early magmatic stage. Platinum group elements, Fe, and part of sulfur might also be carried by the magmas from the source to a shallow level of the crust. The occurrence of sulfide microinclusions indicates that the

magmas were somewhat oversaturated with sulfide during the early magmatic stage. The metals might, at least in part, be carried to 6–10km deep, a depth of the second-stage emplacement of the magmas, where they became saturated with water. Copper concentrations in the magmas might somewhat be controlled by the composition and structure of the melts (Feiss, 1978, 1980).

During the late magmatic stage extracting copper from the melts might be a critical controlling factor over the copper mineralizations. The high correlation coefficients between each of Cu, Au, Ag and F (Tab.6–11) suggest that the ore-forming material might be derived from the same phlogopite-bearing fertilized source as the magmas; while higher correlation coefficients between each of Cu, Au, Ag and Cl (Tab 6–11) further indicate a close relationship between activity of chloride-rich hydrothermal fluid and the copper mineralizations. The hydrothermal fluid equilibrated with crystallizing quartz phenocrysts of Angkenong body, by analyses of fluid phase inclusions, contained as high as 9.96*m* chloride, giving a partition coefficient of copper between vapor and the melt phase about 91.6, thus a hydrothermal fluid containing over 1800 ppm copper could be separated from a melt containing 20ppm copper. This proccess could accompany depletion of Na_2O in the solidifing rocks, causing the copper-bearing porphyries relatively higher in K_2O, lower in Na_2O, and oversaturated with Al_2O_3, which could further enhance solubility of copper in the hydrothermal fluid, as OH-ion could be attracted by Al^{3+}, to decrease pH value of the hydrothermal fluid. The strong outpouring and escape of the fluid at the post-magmatic stage were responsible for both producing numerous cracks within the porphyries to precipitate copper in the fluid and recycling the process.

Physicochemical marks of copper mineralizability: 1) the copper-bearing magmas fall into deep source derived, high liquidus temperature, and relatively higher oxygen fugacity type, and underwent a wide span of crystallizing temperature; 2) during the early magmatic stage the copper-bearing magmas were under higher sulfur fugacity, had higher solubility of sulfur, and might be oversaturated with sulfide, which would cause the activity of FeO to decrease with crystallization of the magmas; 3) during the late magmatic stage the magmas were strongly oversaturated with water, leading hydrothermal fluid containing copper to be separated from the magmas, and outpoured to precipitate copper sulfide, and the process to be recycled; 4) the granite porphyries with relatively higher K_2O/Na_2O ratio and Al_2O_3 oversaturated are of higher potentiality to host porphyry copper deposits.

XII. CONCLUDING REMARKS

1. The granites in the Yulong porphyry copper belt were formed on the tectonic environment of Indonisian volcanic arc related to subduction of the Paleo-Tethysian ocean plate along Jinshajiang, and fall into VAG-type granitoid. Distributed area of the porphyry copper belt is controlled by the magmatic processes in the inherited island arc.

2. Locations of the porphyry bodies and related copper ore deposits are controlled by